Journal of Catalysis **196,** 207–211 (2000)
doi:10.1006/jcat.2000.3047, available online at http://www.idealibrary.com on IDEAL®

DFT Study of the Adsorption and Dissociation of Methanol on NiAl (100)

Lawrence T. Sein, Jr.[1] and Susan A. Jansen

Department of Chemistry, Temple University, Philadelphia, Pennsylvania 19122

Received September 29, 1999; revised March 13, 2000; accepted August 28, 2000

The adsorption of methanol on the (1 : 1) nickel/aluminum (100) surface is modeled by quantum mechanical calculations on a small cluster, using hybrid Hartree–Fock/density functional theory. The enthalpy of adsorption at the limit of zero coverage is calculated for the high-symmetry sites. The importance of tipping of the prevalent methoxy radical species to C–O bond scission is examined. A new mechanism for dissociation is proposed, which is in excellent agreement with experimental determinations of the energy of activation for dissociation. Comparisons are made to similar reactions on Al (100). © 2000 Academic Press

Key Words: **bimetallic catalysis; DFT; methanol; NiAl.**

INTRODUCTION

Since Sinfelt (1–3) introduced the concept of bimetallic catalysts, much research has been devoted to understanding the structure, stability, and reactivity of alloyed metals and secondary metal effects in a variety of catalytic model systems. Systems based on Cu/Ru (3–5), Cu/Zn (6), and Ni/Cu (2, 7, 8) have been investigated extensively. Transition metal carbides (9) have been investigated for their unique surface properties. In many cases a secondary species not present at the surface can define the surface chemistry of the particular system. For bimetallic systems, most studies have focused on transition metal alloys or epitaxial deposition of a secondary metal on a single crystal metal surface. To assure surface stability, alloying metals or size-matched metals are used to limit tensile strain and promote surface stability. The electronic nature demonstrated by the surface is usually a hybrid of the alloying metals.

Transition metal aluminides offer an interesting contrast. They are stable alloys with well-defined surfaces (10). They can be prepared from a variety of transition metals, including titanium, iron, and nickel (11–16). These three metals differ significantly in electronegativity, *d*-orbital occupation, and the electronic character of the *d* states. As transition metals, they form six-coordinate octahedral species. In contrast, aluminum, a main group metal, is very electropositive. Aluminum frequently forms tetrahedral complexes with electronegative species (17–22). The most easily manufactured (100) surface of the binary aluminides is the one that is aluminum terminated, with the transition metal somewhat "exposed" in the fourfold site in the second layer. Both species may have an active role in the surface chemistry.

Studies on the catalytic activities of the aluminum-terminated surfaces have shown that the surface reactivity for each is unique with respect to a series of complex reactions, including the decomposition of methanol and methyl halides. The reaction of methanol is a well-studied reaction for many transition metal, metal oxide, and metal carbide surfaces (9, 23–36). These reactions are of considerable economic importance to both industrial manufacturing and synthetic fuels production, as they relate to the production of synthesis gas (37, 38) and Fischer–Tropsch chemistry. For highly active transition metal surfaces, formaldehyde is a common product (33). For less active transition metal surfaces and carbides, methanol is "deprotonated" to a methoxy radical without further reaction. In some cases, methyl radicals produced at the surface couple to form ethane. Clearly, the utility of any catalyst requires a clear understanding of the surface activity and the operative catalytic mechanism occurring at the surface.

METHODS

Since experiments strongly confirm that, at elevated temperatures, the prevalent methanol species on the surface is the methoxy radical, all calculations were done using this radical (39). Theoretical discussions of the deprotonation of methanol at the hydroxyl are numerous (9, 32–34, 39). The use of the radical $MeO^{\cdot}$, as opposed to the anion, is done largely for computational convenience (40). The (100) surface (Fig. 1) was simulated by a cluster of 14 atoms, 6 aluminum atoms both on the surface and at the third layer, and 2 nickel atoms below the hollows (as the second layer). The Ni–Ni and Al–Al nearest neighbor distance (CsCl structure) is 2.904 Å. For the purposes of the calculations, the spin state of the cluster was considered a singlet, with the nickel atoms antiferromagnetically

---

[1] To whom correspondence should be addressed. E-mail: lsein@thunder.temple.edu.

0021-9517/00 $35.00

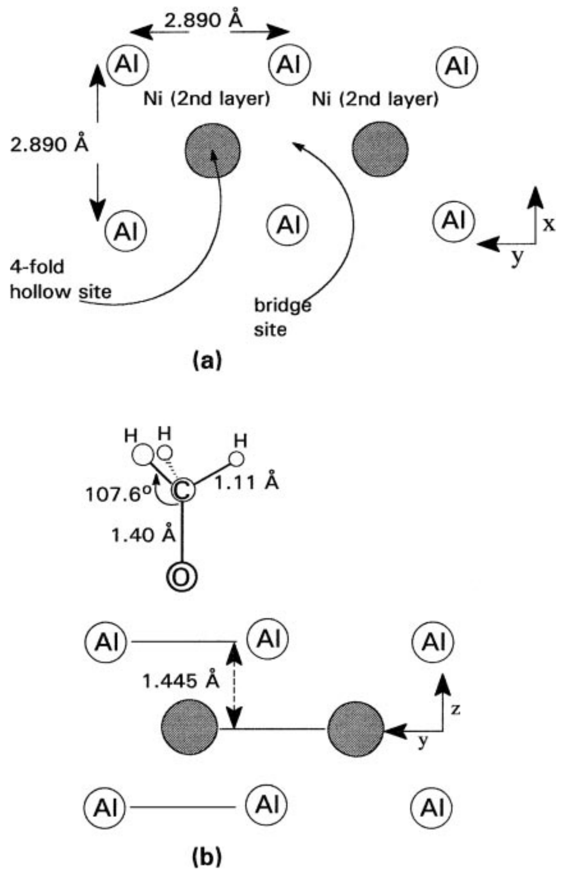

FIG. 1. NiAl (100) cluster model used for calculations, top view (a) and side view (b), showing methoxy at fourfold hollow.

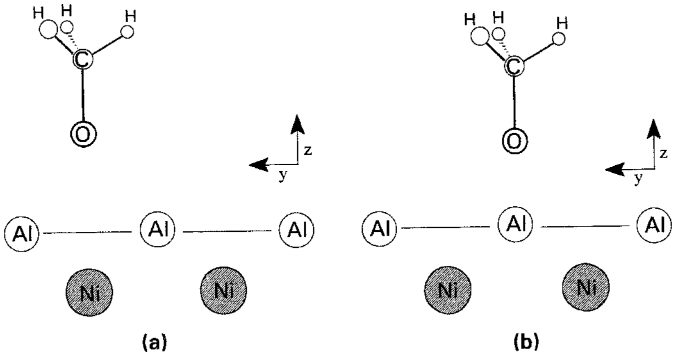

SCHEME 1

coupled. The geometry of the methoxy radical was optimized using the B3LYP functional and the 6-311++G(2d,p) basis set within the Gaussian 94 (41) suite of programs. A series of trial calculations was performed using clusters either enlarged by additional aluminum atoms, or else terminated along all nonsurface planes by hydrogen atoms. This was done to address the concern that unsaturation of the aluminum valences would decrease the accuracy of the calculation. In each case, the results were entirely consistent with those from the 14-atom (Ni_2Al_{12}) cluster. The cluster model used in the calculations has the same symmetry and density of states as would an infinite lattice model with a more truncated unit cell.

Single-point energies were computed using the B3LYP/6-311G(2d,p) basis set. The B3LYP density functional key word corrects the Hartree–Fock energy to account for the effects of electron–electron repulsion, correlation, and exchange. Density functional theory provides high accuracy at minimal cost (42). In contrast to the effective core potential (ECP) methods (43), which lump the contributions of the inner electrons into a single electrostatic term, the calculations herein described in this part of the work explicitly account for all electrons. While ECP methods are essential to modeling elements in which relativistic effects are critical, these effects are of minor importance in nickel.

Single-point energy calculations were performed for the methoxy radical at intervals of 0.1 Å during its trajectory toward the surface during adsorption. Both the trajectory and the radical itself were kept normal to the surface. Trajectories toward both the fourfold hollow (Scheme 1a) and twofold bridge sites (Scheme 1b) were computed. Calculations of "tipping" were done by tilting the C–O bond axis relative to the plane of the surface, from 0° (normal) to 90° (Scheme 2a, b). Two unique tipping trajectories were employed, one with the oxygen atom in the hollow site and the other with the oxygen atom in the bridge site. During the tipping of the methoxy radical, the oxygen atom itself was not moved, and all bond angles (except that of the C–O bond to the surface) and bond lengths were left unchanged (*vide infra*).

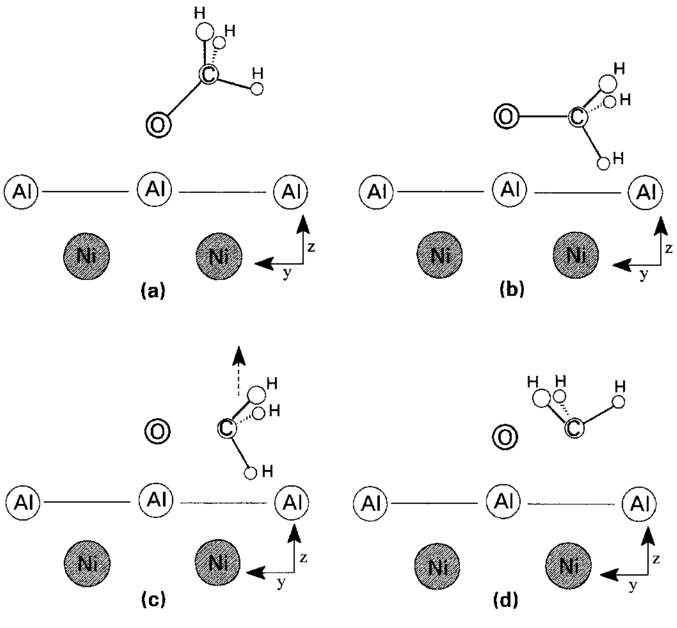

SCHEME 2

TABLE 1

Calculated Carbon–Oxygen Bond Lengths for Methoxy Adsorbed on NiAl (100)[a]

Oxygen–nickel distance	Hollow	Bridge
2.3	1.5179	
2.4	1.5052	
2.6		1.4685
2.7	1.4809	1.4629
2.8	1.4741	1.4567
3.0		1.4523
3.2	1.4558	1.4493

[a] As calculated at B3LYP/6-31G on all atoms except nickel, for which B3LYP/CRENBL ECP was used. All distances in Å.

To simulate the dissociated products, energy calculations were performed with the oxygen atom in either the hollow or the bridge site and the methyl group free to move (normal to the surface) directly off the surface (Scheme 2c) from either the bridge site (when the O was in the hollow) or from the hollow (when the O was in the bridge). In these calculations, the methyl group was oriented with the plane of the hydrogen atoms *normal* to the surface. Other calculations (not shown) with the plane of the hydrogen atoms of the methyl group parallel to the surface (Scheme 2d) are much higher in energy. The preference for the methyl group orientation is the same whether or not there is an adjacent oxygen, suggesting that a residual amount of C–O bonding is not responsible for this preference. Atomic charges on atoms and overlap populations were computed using the Mulliken method at the B3LYP/6-311G(2d,p) level.

Trial calculations were performed in which the methoxy radical was allowed to "relax" (change bond lengths, angles). Here, the 6-31G basis set was used for all atoms except nickel, for which the CRENBL ECP (44, 45) was used. Zero-point and enthalpic corrections were performed using the same sets for several (but not all) of the geometries since such corrections, being "numeric," were both computationally demanding and simultaneously less accurate than "analytical" ones, and varied no more than by 3 kcal mol^{-1}. In each case, the minima found were extremely close to the fixed geometries employed in this study (Table 1). Furthermore, in the region of the minima, the potential energy surface of the radical was so shallow that the available thermal energy at 298 K (and above) would ensure that few molecules would actually be in the potential energy well.

RESULTS

Potential energy curves for the trajectory of the methoxy radical normal to the surface are shown in Fig. 2. Contrary to expectation, the lowest energy site is the bridge site. Since the difference in energy between the two sites is ∼15 kcal mol^{-1}, we can assume that, at low coverage, the barrier to diffusion is also 15 kcal mol^{-1} (39), which is much larger than the barrier found on Al(100) (46). Other calculations, not shown, have demonstrated that the on-top adsorption site is even higher in energy than either the hollow or the bridge.

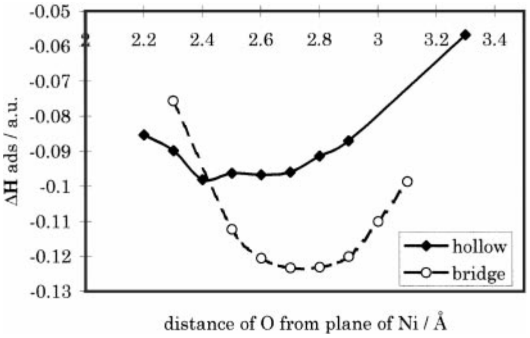

FIG. 2. Enthalpy of adsorption of methoxy at hollow and bridge sites of NiAl (100), calculated at B3LYP/6-311G(2d,p).

In Table 2 are the partial atomic charges on the carbon, oxygen, and nickel atoms at the bridge adsorption site. The overlap populations for the C–O and C–N (hollow) bonds are listed in Table 3. For the methoxy radical at both the hollow and the bridge sites, initial chemisorption decreases the C–O overlap from the gas phase value. This is as would be expected for bonding to a Group 13 (electron-deficient) atom (47). As the radical tips, the C–O overlap population decreases, consistent with C–O bond scission.

DISCUSSION

It has been suggested that the C–O bond becomes so weakened upon adsorption that the methyl group ejects upward upon heating. Three reasons have been given to justify this hypothesis: first, there is donation from the Fermi level of the NiAl metal to an antibonding (σ^*) M.O.

TABLE 2

Atomic Charges of Methoxy on NiAl (100), Tipped at Bridge Site

Tip angle (°)	Ni	O	C
10	0.1188	−0.8814	−0.2232
20	0.1226	−0.8709	−0.2150
30	0.1515	−0.8575	−0.2216
40	0.1350	−0.8348	−0.2225
50	0.1201	−0.8179	−0.2184
60	0.0857	−0.7838	−0.2194
70	0.0751	−0.7410	−0.2840
80	0.0661	−0.7050	−0.4461
85	0.0675	−0.6864	−0.5351
90	0.0507	−0.6727	−0.6372

TABLE 3

Overlap Populations of Methoxy on NiAl (100) Tipped at Bridge Site

Tip angle (°)	C–O overlap	Ni–C overlap
10	0.1423	0.0138
20	0.1384	0.0157
30	0.1444	0.0216
40	0.1366	0.0283
50	0.1344	0.0278
60	0.1344	−0.0400
70	0.0785	−0.3144
80	−0.0052	−0.5177
85	−0.0505	−0.5122
90	−0.0838	−0.4747

of the methoxy, thus promoting dissociation (48); second, the enthalpy of bond formation between the oxygen and the metal is large enough to overcome the bond strength of the C–O (49); and third, the weakness of alkyl oxygen bonds has been demonstrated by the abstraction of hydrogen from methane by metal oxides in the gas phase (50). None of these arguments seem convincing.

The σ^* orbital of methanol (or methoxy) is much too high in energy to interact with the Fermi level of aluminum itself (9); the Fermi level of NiAl (100) is even lower. Work function of NiAl (100) = 4.6 eV (48) and of Al (100) = 4.51 eV (21). Note that Fermi level and work function are *inversely* related. Also, no matter how strong the bond might be between the methoxy oxygen atom and a metal atom, the orbitals (and electrons) on the oxygen atom are *nonbonding*, so their use elsewhere in bonding has little effect on the methyl–oxygen bonding. While it is true that metal oxides can abstract hydrogen from methane, it is not exactly clear how this reflects upon the strength of C–O bonds, as there are no evident C–O bonds in the gas phase reaction of metal oxides and methane.

TPD experiments on NiAl (100) determined the energy of activation for the ejection of methyl from methanol to be approximately 35 kcal/mol^{-1} (48) [obtained by substitution into equation (39)]. Given the marked preference of the adsorbed methoxy radical for the bridge site over the hollow, it was not surprising that the calculated energy of activation for tipping at that site was >100 kcal mol^{-1}.

We therefore calculated the energetics of tipping at the bridge site toward a hollow, and these results are much closer to the experimental results (Fig. 3). The steady decrease in the C–O overlap population is consistent with bond weakening. The repolarization of the C–O bond, with the increase of negative charge on carbon and decrease of negative charge on oxygen and positive charge on nickel, confirms that tipping is sufficient to dissociate the C–O bond and to form a C–Ni bond. The energy of activation for dissociation is computed (*ab initio*) at ~40 kcal mol^{-1}.

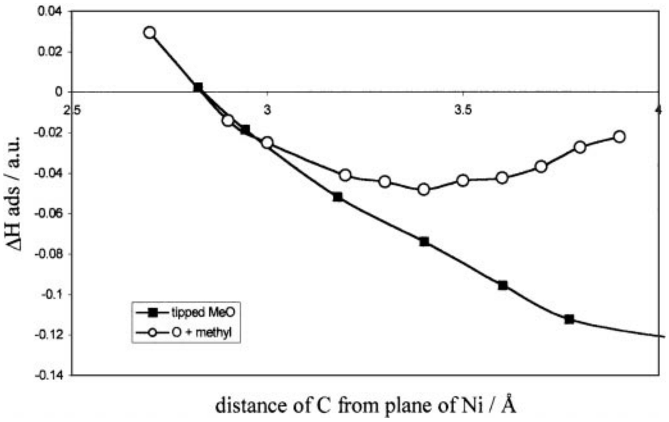

FIG. 3. Enthalpy of adsorption of methoxy, tipped at bridge, and dissociation products, calculated at B3LYP/6-311G(2d,p).

This value is slightly higher than the result obtained from the TPD data. However, it must be kept in mind that the computation of energies of activation from TPD data are limited by three factors: the assumption of the pre-exponential factor to be exactly 10^{13} s^{-1}, the disregard of the broadness of the TPD peak, and nonlinearities in the heating rate. A difference in the presumed pre-exponential factor of 3 orders of magnitude leads to a difference of 3 kcal mol^{-1} in the energy of activation. The TPD data upon which this determination were based involve a peak that is 150 K wide (48). Lastly, the published heating rate of 7 K s^{-1} is extremely difficult to maintain.

An important point, somewhat overlooked in the analysis so far, is that of geometry. Adsorption at the bridge allows tipping of the (electron-rich) methoxy toward the (electron-poor) fourfold hollow. Thereby electrostatic repulsion is minimized (51). This is not the complete answer, however, since TiAl and FeAl binary surfaces have essentially the same geometry as NiAl, but have energies of activation for dissociation that are quite smaller.

CONCLUSION

It is possible to determine the site preference of chemisorption of the methoxy radical upon the NiAl (100) surface, along with a quantitatively accurate enthalpy of adsorption. Methanol prefers the twofold bridge site to the fourfold hollow site, even more strongly than in the case of Al(100) (46). While tipping from either adsorption site seems to weaken the C–O bond, the energy of activation for tipping is much smaller for the bridge-adsorbed methoxy, where a C–Ni bond is formed. There is close agreement of the calculated energy of activation of tipping with the (experimental) energy of activation for the dissociation reaction of methanol on NiAl. This suggests that the tipping of methoxy, just as in the case of Al (100), is the rate-determining step in the dissociation of methanol on NiAl

(100). The interaction between the adsorbate and the secondary metal (though not even at the surface) is necessary to promote dissociation.

Units. 1 hartree (a.u.) equals 627.5095 kcal mol^{-1}.

ACKNOWLEDGMENTS

President Dr. Peter J. Liacouras is gratefully acknowledged for allowing us access to the Temple University DEC Alpha-4019 used for all computations in this paper. L.T.S. thanks the graduate school of Temple University for a dissertation completion fellowship.

REFERENCES

1. Sinfelt, J. H., *J. Catal.* **29**, 308 (1973). Sinfelt, J. H., *Catal Rev.–Sci. Eng.* **9**, 147 (1974); Sinfelt, J. H., “Bimetallic Catalysis-Discoveries, Concept and Applications.” Wiley, New York, 1983.
2. Sinfelt, J. H., *Acc. Chem. Res.* **10**, 15 (1977).
3. Sinfelt, J. H., *Acc. Chem. Res.* **20**, 134 (1987).
4. Christmann, K., Ertl, G., and Shimizu, H., *J. Catal.* **61**, 397 (1980).
5. Jansen, S. A., Palmieri, M., Gomez, M., and Lawrence, S., *J. Catal.* **163**, 262 (1996).
6. Von Heidenstam, O., Johansson, A., and Westman, S., *Acta Chem. Scand.* **22**, 653 (1968).
7. Clarke, J. K. A., *Chem. Rev.* **75**, 291 (1975).
8. Cale, T. S., and Richardson, J. T., *J. Catal.* **79**, 378 (1983).
9. Jansen, S. A., and Hoffmann, R., *Surf. Sci.* **197**, 474 (1988).
10. Davis, H. L., and Noonan, J. R., *in* “The Structure of Surfaces II” (J. F. van der Veen and M. A. van Hove, Eds.). pp. 173–195. Springer-Verlag, New York, 1987.
11. Chaturvedi, S., and Strongin, D. R., *Langmuir* **13**, 3162 (1997).
12. Zhang, Y., Wang, Y., Chu, W., Hsiao, C., and Thompson, A. W., *Scr. Metall. Mater.* **26**(6), 925 (1992).
13. Sheu, B. R., and Strongin, D. R. *Langmuir* **10**, 1801 (1994).
14. Sheu, B. R., and Strongin, D. R., *J. Catal.* **154**, 379 (1995).
15. Grillo, M. E., *J. Chem. Phys.* **97**, 7786 (1992).
16. (a) Jaeger, R. M., Kuhlenleck, H., Freund, H. J., Wittis, M., Hoffman, W., Frandy, R., and Ibach, H., *Surf. Sci.* **251**, 866 (1991). (b) Nepijko, S. A., Klimenkov, M., Adelt, M., Kuhlenbeck, J., Schlogl, R., and Freund, H.-J., *Langmuir* **15**(16), 5309 (1999). (c) Chaturvedi, S., and Strongin, D. R., *J. Phys. Chem. B* **102**, 2970 (1998). (d) Chaturvedi, S., and Strongin, D. R., *Langmuir* **13**, 3162 (1997). (e) Risse, T., Hill, T., Beckendorf, M., Katter, U. J., Schlienz, H., Hamann, H., and Freund, H.-J., *Langmuir* **12**, 5512 (1996).
17. Bargeron, C. B., Hall, B. H., and Jette, A. N., *Surf. Sci.* **120**, L487 (1982).
18. Brune, H., *J. Chem. Phys.* **99**, 2128 (1993).
19. Kondoh, H., Hara, M., Domen, K., and Nozoye, H., *Surf. Sci.* **208**, L287 (1992).
20. Lauderback, L. L., Lynn, A. J., Waltman, C. J., and Larsen, S. A., *Surf. Sci.* **243**, 323 (1991).
21. Schoechling, J., Buhnan, K. P., and Hon, K. M., *Surf. Sci.* **324**, 113 (1995).
22. Winkler, A., Pozgainer, G., and Rendulic, K. D., *Surf. Sci.* **251**, 886 (1991).
23. Chen, J. G., Beebe, T. P., Jr., Crowell, J. E., and Yates, J. T., Jr., *J. Am. Chem. Soc.* **109**, 1726 (1987).
24. Basu, P., Chen, G., Ng, L., Colaianni, M. L., and Yates, J. T., Jr., *J. Chem. Phys.* **89**(4), 2406 (1988).
25. Dabrowski, A., Bogillo, V. I., and Shkilev, V. P., *Langmuir* **12**, 936 (1996).
26. Kovacs, I., and Solymosi, F., *J. Phys. Chem. B* **101**, 5397 (1997).
27. Legarski, B. R., and Dubois, L. H., *Surf. Sci.* **262**, L129 (1992).
28. Ma, M. C., Brown, T. C., and Haynes, B. S., *Surf. Sci.* **297**, 312 (1993).
29. Paul, A., Yang, M. X., and Bent, B. E., *Surf. Sci.* **297**, 327 (1993).
30. Rogers, J. W., Jr., Hance, R. L., and White, J. M., *Surf. Sci.* **100**, 388 (1980).
31. Shen, J., Spiekwak, B. E., and Dumesic, J. A., *Langmuir* **13**, 2735 (1997).
32. Shustorovich, E., and Bell, A. T., *Surf. Sci.* **268**, 397 (1992).
33. Tatibouet, J. M., *Appl. Catal. A* **148**, 213 (1997).
34. Tindall, I. F., and Vickerman, J. C., *Surf. Sci.* **149**, 597 (1985).
35. Weigel, J., Koeppel, R. A., Baiker, A., and Wokaun, A., *Langmuir* **12**, 5319 (1996).
36. Whitten, J. E., Young, C. E., Pellin, M. J., Green, D. M., and Jones, P. L., *Surf. Sci.* **241**, 73 (1991).
37. Jacobs, H., Pollok, S., and Golinski, F., *Z. Anorg. Allg. Chem.* **620**, 1213 (1994).
38. Schnick, W., and Lucke, J., *Z. Anorg. Allg. Chem.* **588**, 19 (1990).
39. Benziger, J. B., *in* “Metal-Surface Reaction Energetics: Theory and Applications to Heterogeneous Catalysis, Chemisorption, and Surface Diffusion” (E. Shustorovich, Ed.), p. 92. New York, 1991.
40. See though: Zeroka, D., and Hoffmann, R., *Langmuir* **3**, 553 (1986) for a more theoretical justification.
41. Frisch, M. J., Trucks, G. W., Schlegel, H. B., Gill, P. M. W., Johnson, B. G., Robb, M. A., Cheeseman, J. R., Keith, T., Petersson, G. A., Montgomery, J. A., Raghavachari, K., Al-Lahan, M. A., Zakrewski, V. G., Ortiz, J. V., Foresman, J. B., Cioslowski, J., Stefanov, B. B., Nanayakkara, A., Challacombe, M., Peng, C. Y., Ayala, P. Y., Chen, W., Wong, M. W., Andres, J. L., Replogle, E. S., Gomperts, R., Martin, R. L., Fox, D. J., Binkley, J. S., Defrees, D. J., Baker, J., Stewart, J. P., Head-Gordon, M., Gonzalez, C., Pople, J. A., Gaussian 94. Revision D.1, Pittsburg, PA, 1995.
42. Foresman, J. B., and Frisch, Æ, *in* “Exploring Chemistry with Electronic Structure Methods,” p. 6. Gaussian, Inc., Pittsburgh, PA, 1995.
43. Siegbahn, P. E. M., and Wahlgen, U., *in* “Metal-Surface Reaction Energetics: Theory and Applications to Heterogeneous Catalysis, Chemisorption, and Surface Diffusion” (E. Shustorovich, Ed.), p. 1. VCH, New York, 1991.
44. Basis sets were obtained from the Extensible Computational Chemistry Environment Basis Set Database, Version 1.0, as developed and distributed by the Molecular Science Computing Facility, Environmental and Molecular Sciences Laboratory, which is part of the Pacific Northwest Laboratory, P.O. Box 999, Richland, Washington 99352, USA, and funded by the U.S. Department of Energy. The Pacific Northwest Laboratory is a multiprogram laboratory operated by Battelle Memorial Institute for the U.S. Department of Energy under contract DE-AC06-76RLO 1830. Contact David Feller or Karen Schuchardt for further information.
45. Pacios, L. F., and Christiansen, P. A., *J. Chem. Phys.* **82**, 2664 (1985).
46. Sein, L. T., Jr., and Jansen, S. A., *J. Phys. Chem. B* **102**, 2415 (1998).
47. Douglas, B., McDaniel, D., and Alexander, J., *in* “Concepts and Models in Inorganic Chemistry,” p. 598. Wiley, New York, 1994.
48. Sheu, B. R., Doctoral dissertation, State University of New York at Stoneybrook, 1994.
49. Chen, D. A., and Friend, C. M., *J. Phys. Chem. B* **101**, 5712 (1997).
50. Shiller, P., and Anderson, A. B., *J. Phys. Chem.* **95**, 1396 (1991).
51. We are thankful to a reviewer for reminding us of the importance of geometric factors.